Article

Not peer-reviewed version

Determination of Surface Physicochemical Parameters of Styrene–Divinylbenzene Copolymer Modified by 5-Fluouracil Using Inverse Gas Chromatography

Tayssir Hamieh * and Vladimir Yu Gus'kov

Posted Date: 22 April 2025

doi: 10.20944/preprints202504.1864.v1

Keywords: Modified copolymer; pharmaceutical; surfaces and interfaces; Hamieh thermal model; surface energy; Surface thermodynamic parameters; supramolecular structure doi:10.20944/preprints202504.1864.v1

Article

Determination of Surface Physicochemical Parameters of Styrene–Divinylbenzene Copolymer Modified by 5-Fluouracil Using Inverse Gas Chromatography

Tayssir Hamieh [1,2,*] and Vladimir Yu Gus'kov [3]

[1] Faculty of Science and Engineering, Maastricht University, P.O. Box 616, 6200 MD Maastricht, The Netherlands
[2] Institut de Science des Matériaux de Mulhouse, Université de Haute-Alsace, CNRS, IS2M UMR 7361, F-68100 Mulhouse, France
[3] Laboratory of Materials, Catalysis, Environment and Analytical Methods (MCEMA), Faculty of Sciences, Lebanese University, Beirut P.O. Box 6573/14, Lebanon
[4] Faculty of Science and Technology, Ufa University of Science and Technology, Ufa P.O. 450076, Russia
* Correspondence: t.hamieh@maastrichtuniversity.nl

Abstract: This paper is devoted to the determination of the surface properties of styrene–divinylbenzene (S-DVB) copolymer modified by 5-fluouracil (5-FU). This new research constitutes a further extension of previous works carried out on S-DVB copolymer modified by 5-Hydroxy-6-methyluracil and melamine. The vital interest of the system realized by the modification of S-DVB by 5-FU due to its applications in many important chemical, biochemical, pharmaceutical, and engineering processes influenced our choice to strengthen this type of study and to fill the gap that exists in this field. The powerful inverse gas chromatography (IGC) technique at infinite dilution was used to determine the various surface thermodynamic parameters of S-DVB copolymer modified by 5-FU by varying the temperature and the modifier percentage. The experimental chromatographic measurements of the retention time and volume of the adsorbed organic solvents on the solid surfaces constituted the key with which we open all the surface interaction parameters between the solvents and the solid materials. The dispersive and polar free energies, the London dispersive surface energy, the various polar acid-base surface energies, and the Lewis acid-base parameters of the modified copolymer were determined using the Hamieh thermal model and the new method allowing the separation between the dispersive and polar interaction energy. The new results were compared to those obtained with the S-DVB copolymer modified by other supramolecular structures such as melamine and 5-Hydroxy-6-methyluracil.

Keywords: Modified copolymer; pharmaceutical; surfaces and interfaces; Hamieh thermal model; surface energy; Surface thermodynamic parameters; supramolecular structure

1. Introduction

Styrene–divinylbenzene (S-DVB) copolymers are widely recognized for their structural stability, tunable porosity, and versatility in industrial and biomedical applications [1-4]. The modification of Styrene–divinylbenzene copolymers with 5-Fluorouracil (5-FU) has garnered significant attention due to its potential applications in drug delivery, biomedical engineering, and catalysis [5,6]. Indeed, the incorporation of 5-FU, a chemotherapeutic agent, into these copolymers introduces functional groups that enhance their surface properties, making them suitable for targeted drug delivery and controlled release systems [7-11]. Several surface properties are involved by the modified copolymers. The modification with 5-FU alters the London dispersive and polar free energies of the copolymer, enhancing its interaction with polar and non-polar molecules. This property is crucial for adsorption and separation processes. While the functional groups such as carbonyl and amine groups

doi:10.20944/preprints202504.1864.v1

through 5-FU modification increase the reactivity of the copolymer surface, enabling further functionalization and improving its compatibility with biological systems [12]. The incorporation of 5-FU also affects the porosity and surface morphology of the copolymer, optimizing it for applications such as controlled drug release and catalysis. Enhanced porosity allows for better drug encapsulation and release profiles [8-11,13]. On the other hand, the enhanced biocompatibility of the modified copolymer makes it suitable for biomedical applications, including implants and localized drug delivery systems [6]. Nevertheless, the modification often improves the thermal stability of the copolymer, ensuring its structural integrity during high-temperature processes [14]. This is particularly important for applications in catalysis and industrial processing [15]. Several studies have shown that the supramolecular structure formed by 5-FU on the copolymer surface contributes to increased sorption activity [16]. This is particularly useful in applications requiring selective adsorption, such as chromatography and purification. Whereas, the shielding effect of fluorine atoms in 5-FU reduces surface polarity, can influence interactions with polar solvents and molecules [16,17]. The modified copolymer also influences the surface charge of the copolymer and the Lewis acid-base characteristics, which enhance its ability to interact with specific molecules [18].

Several studies were devoted to study the modification of S-DVB copolymers by modifiers such as 5-Fluouracil and realized supramolecular structures used in many industrial applications [19-27]. However, there is an incredible lack in knowledge of the surface thermodynamic properties of S-DVB copolymer modified by 5-fluouracil, and especially, in the London dispersive and polar surface properties of these materials.

In two recent papers [28,29], we determined the various surface properties of Styrene–divinylbenzene copolymer modified respectively by melamine and 5-hydroxy-6-methyluracil (HMU) by varying the modifier percentage and the temperature using the powerful inverse gas chromatography (IGC) at infinite dilution [30-67]. Indeed, this IGC technique allowed determining the net retention volume Vn of the various organic solvents adsorbed on the S-DVB modified by melamine [28] and HMU [29] for different percentages. The experimental determination of Vn characteristic of the interaction between the solid materials and n-alkanes and polar organic molecules led to the values of all surface thermodynamic parameters of adsorption [46-49,54,64-67], particularly, the free energy of adsorption $\Delta G_a^0(T)$, the London dispersive free energy $\Delta G_a^d(T)$, the free polar energy $\Delta G_a^{sp}(T)$, the Lewis enthalpic acid K_A and base K_D, and the Lewis entropic acid ω_A and base ω_D, the London dispersive surface energy $\gamma_s^d(T)$, the polar (or acid–base) surface energy γ_s^p, and the total surface energy γ_s of the modified copolymers [28,29]. The results obtained with these two systems are very promising in the field of surface chemistry of the modified copolymers.

We aim in this study to fill the gaps and lack of literature in this area by investigating the surface thermodynamic properties of S-DVB copolymers modified by 5-FU at different concentrations using IGC technique at infinite dilution using our new methodology that proved to be the best suited to the study of the physicochemical properties of solid surfaces [54,64-67]. Indeed, the new proposed methodology has remedied the various errors encountered in the literature over the last fifty years and better characterized the surface properties of solid materials using IGC technique at infinite dilution. A comparison of the new results on S-DVB copolymers modified by 5-FU obtained in this work was carried out with those previously determined by modification of S-DVB by melamine and HMU [28,29].

2. Materials and Methods

2.1. Materials and Technique

In this study, the various model organic solvents and the S-DVB copolymers were identical to those employed in two recent papers [28,29], while the 5-FU modifier was purchased from Vecton, St. Petersburg, Russia, using the same experimental protocol. The experimental measurements of the net retention time and retention volume of the adsorbed organic solvents on the system S-DVB / 5-FU at different percentages were obtained from the Chromos GC-1000 chromatograph (from

Chromos, Russia) equipped with a flame ionization detector (FID) used with the same previous procedure [28,29].

2.2. Thermodynamic Methods

2.2.1. Polar Free Energy of Adsorption and Lewis Acid-Base Equations

The experimental determination of the net retention volume of the adsorbed molecules led to the values of the free energy of adsorption at various temperatures using the fundamental thermodynamic equation of inverse gas chromatography:

$$\Delta G_a^0(T) = -RTlnVn + C(T) \quad (1)$$

where T is the absolute temperature, R the perfect constant gas, and $C(T)$ a constant parameter of adsorption.

Knowing that $\Delta G_a^0(T)$ is divided into two contributions: the first one concerns the London dispersive energy $\Delta G_a^d(T)$ obtained from the interaction between the modified copolymer and the non-polar solvents such as the n-alkanes (Equation 2) and the second term represents the free polar energy $\Delta G_a^p(T)$ obtained by Hamieh method [66,67]:

$$\Delta G_a^d(T) = -\frac{\alpha_{0S}}{H^6}\left[\frac{3\mathcal{N}}{2(4\pi\varepsilon_0)^2}\mathcal{P}_{SX}\right] \quad (2)$$

where $\mathcal{N}$ is the Avogadro number, ε_0 the dielectric constant of vacuum, α_{0S} the deformation polarizability of the solid material denoted by S, H the separation distance between the organic solvent and the solid surface, and $\mathcal{P}_{SX}$ an interaction parameter used by Hamieh [66,67] as a chromatographic index (Equation 3):

$$\mathcal{P}_{SX} = \frac{\varepsilon_S\ \varepsilon_X}{(\varepsilon_S +\ \varepsilon_X)}\alpha_{0X} \quad (3)$$

where α_{0X} is the deformation polarizability of the solvent X, and ε_S and ε_X are respectively the ionization energies of the solid and the solvent

The values of $\Delta G_a^p(polar)$ were determined using Equation 4:

$$\Delta G_a^p(T, polar) = RTlnVn\ (T, polar) - RTlnVn\ (T, X_{n.p.}) \quad (4)$$

where $X_{n.p.}$is the geometric point representing the intersection between the straight n-alkanes line with the perpendicular drawn from the point representing the polar probe.

The variations of $\Delta G_a^p(T)$ versus the temperature led to the values of the polar enthalpy $(-\Delta H_a^p)$ and entropy $(-\Delta S_a^p)$ of adsorption obtained using Equation (5):

$$\Delta G_a^p(T) = \Delta H_a^p - T\Delta S_a^p \quad (5)$$

Whereas the Lewis enthalpic (K_A, K_D) and entropic (ω_A, ω_D) acid–base parameters were obtained from Equations (6)::

$$\begin{cases}(-\Delta H^p) = & K_A \times DN' + K_D \times AN' \\ (-\Delta S_a^p) = & \omega_A \times DN' + \omega_D \times AN'\end{cases} \quad (6)$$

where $DN'$and $AN'$are, respectively, the corrected electron donor and acceptor numbers of the polar molecule [64-67].

2.2.2. Surface Energetics of the modified copolymers

The application of the Hamieh thermal model [46,46,57, 64-67] allowed us obtaining the London dispersive surface energy $\gamma_s^d(T)$ of the modified copolymer using Equation 7:

$$RTlnV_n = 2\mathcal{N}a(T)\left[\gamma_l^d(T)\gamma_s^d(T)\right]^{1/2} + \beta(T) \quad (7)$$

Preprints.org (www.preprints.org) | NOT PEER-REVIEWED | Posted: 22 April 2025 doi:10.20944/preprints202504.1864.v1

where $a(T)$ is the surface area of solvents given by Hamieh [46] as a function of the temperature, $\gamma_l^d(T)$ the London dispersive component of the surface energy of the solvent, and $\beta(T)$ a constant depending only on the temperature and the solid material.

If γ_s^p represents the polar surface energy of the S-DVB copolymer, the total surface energy γ_s can be then written as:

$$\gamma_s = \gamma_s^d + \gamma_s^p \tag{8}$$

The Van Oss et al.'s method [36] applied to the modified copolymers led to the values of the Lewis acid γ_s^+, and base γ_s^- surface energies using the $\Delta G_a^p(T)$ and the known surface parameters of ethyl acetate and dichloromethane:

$$\Delta G_a^p(T) = 2\mathcal{N}a(T)\left(\sqrt{\gamma_l^- \gamma_s^+} + \sqrt{\gamma_l^+ \gamma_s^-}\right) \tag{9}$$

The values of γ_s^p can be therefore obtained from Expression (10):

$$\gamma_s^{AB} = \gamma_s^p = 2\sqrt{\gamma_s^+ \gamma_s^-} \tag{10}$$

3. Results

3.1. Variations of the Free Energy of Adsorption

By determining the values of $RTlnV_n(T)$ of different probes adsorbed on the system S-DVB - 5-FU for various temperatures and 5-FU percentages, the results were plotted in Figure 1. Linear variations of $RTlnV_n(T)$ were found (Figure 1) for all solvents and solid materials showing a large difference in the behavior in the values of the free energy of adsorption of the probes and copolymers. Higher energy of interaction was obtained with the modified S-DVB for higher percentage of 5-FU. Figure 1 also showed that the polar solvents exchanged the highest free of adsorption. The highest values of $RTlnV_n(T)$ were obtained in the case of i-butanol and i-propanol. These preliminary results indicate the higher possibility to have more free energy of interaction with S-DVB modified by 5-FU. These observations were confirmed in the next section by the determination of free polar energy of adsorption of the various polar solvents adsorbed on the modified copolymer proving the high potentiality of the use of such copolymers in industrial and pharmaceutical applications that need more polar surface groups in the copolymer structure.

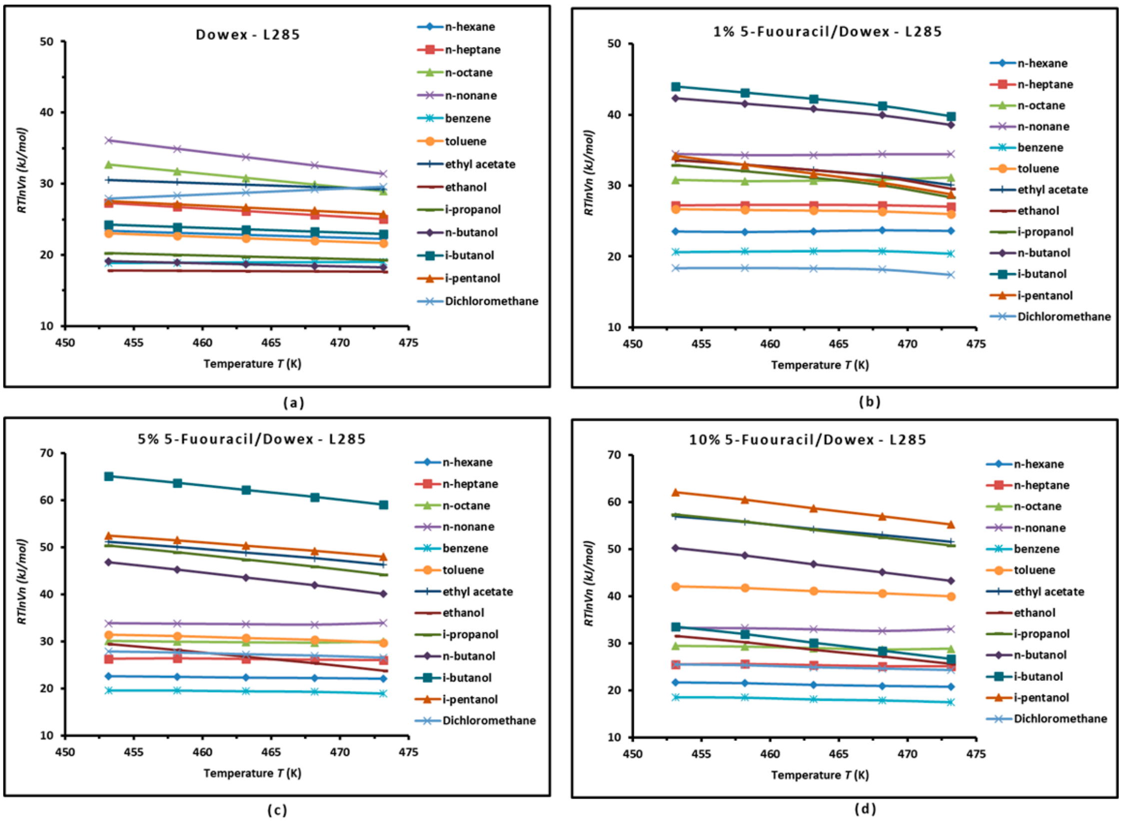

Figure 1. Effect of the percentage of 5-fluouracil modifying the styrene–divinylbenzene copolymer, on the values of $RTlnV_n(T)$ of different adsorbed organic solvents at various temperatures. S-DVB-L-285 (a), 1% of 5-fluouracil (b), 5% of 5-fluouracil (c), and 10% of 5-fluouracil (d).

3.2. Determination of the London Dispersive Surface Energy

The values of $\gamma_s^d(T)$ of the S-DVB / 5-FU systems were determined using Equation (7) for the various modifier percentages at each temperature and applying the Hamieh thermal model [46,47,54,60,64,65]. A decrease of $\gamma_s^d(T)$ was observed in Figure 2a when the temperature increased. However, the London dispersive surface energy of S-DVB copolymer decreased until a 5-FU percentage of 1% and slightly increased for higher percentage of the 5-FU modifier for T =253.15K and 258.13K. An inversion of the tendency was showed in Figure 2b for T =268.15K and 273.13K, where a sharp increase was seen at these temperatures until 1% of 5-FU and then a slight increase was observed for 5% and 10% 5-FU. While a linear increase was observed at a temperature of 263.15K.

The large difference in the values of $\gamma_s^d(T)$ when the 5-FU percentage can be more visualized by giving in Table 1, the various equations of $\gamma_s^d(T)$ of copolymers with other surface thermodynamic parameters by supposing a global linearity of $\gamma_s^d(T)$ versus the temperature.

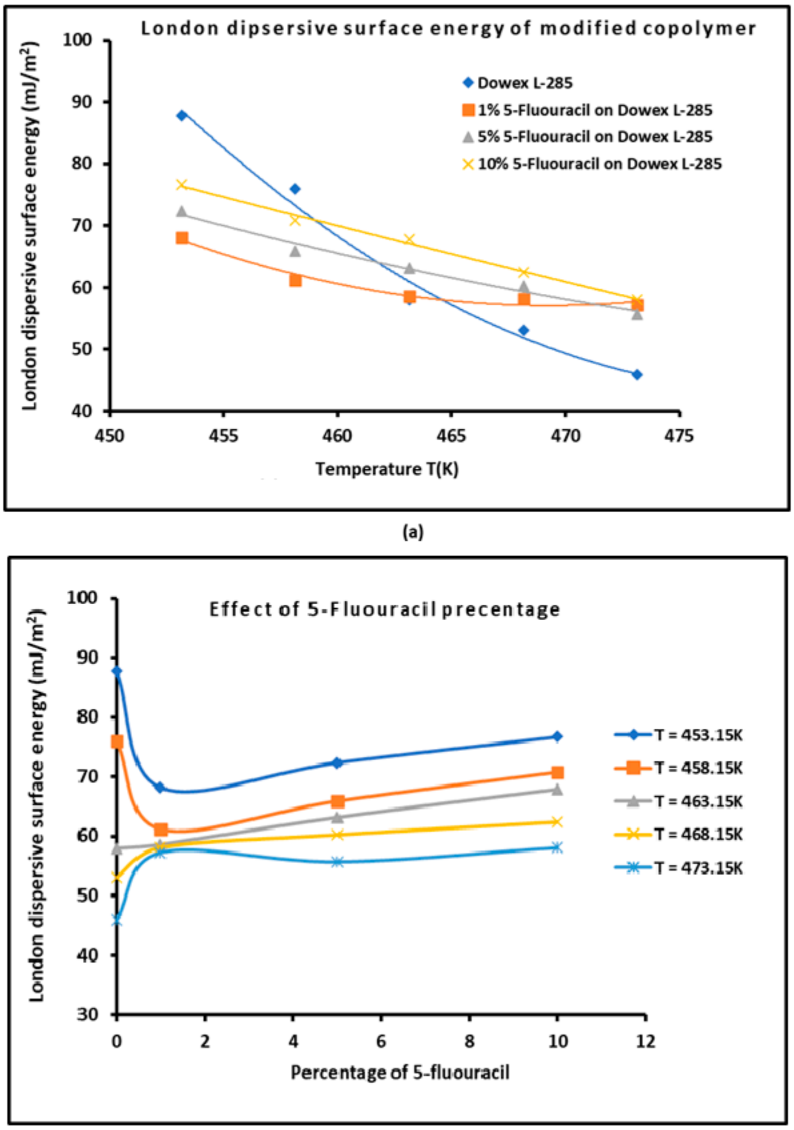

(a)

(b)

Figure 2. Variations of $\gamma_s^d(T)$ of modified S-DVB copolymer versu the temperature (a) and the percentage of 5-fluouracil (b).

Table 1. Linear expressions of $\gamma_s^d(T)$ of S-DVB modified by different percentages of 5-fluouracil (5-FU), regression coefficients, London dispersive surface entropy ε_s^d, and the temperature maximum T_{Max}, using the Hamieh thermal model.

Copolymer	$\gamma_s^d(T)$ (mJ/m²)	R²	$\varepsilon_s^d = d\gamma_s^d/dT$ (mJ m⁻² K⁻¹)	$\gamma_s^d(T=0K)$ (mJ/m²)	T_{Max} (K)
S-DVB	$\gamma_s^d(T)$ = -2.1343 T + 1052.7	0.9543	-2.134	1052.70	493.3
1% 5-FU / S-DVB	$\gamma_s^d(T)$ = -0.4972 T + 290.95	0.8900	-0.497	290.95	585.4
5% 5-FU / S-DVB	$\gamma_s^d(T)$ = -0.7799 T + 424.67	0.9800	-0.780	424.67	544.4
10% 5-FU / S-DVB	$\gamma_s^d(T)$ = -0.9131 T + 490.08	0.9900	-0.913	490.08	536.8

Results in Table 1 proved an increase in absolute value of the London dispersive surface entropy ε_s^d of copolymer, an increase of the extrapolated dispersive surface energy $\gamma_s^d(T=0K)$ at 0K, and a gradual decrease of the maximum temperature T_{Max}. These results can be better understood in Table 2.

Table 2. Linear expressions of ε_s^d, $\gamma_s^d(T=0K)$, and T_{Max} as a function of 5-FU percentage, and the corresponding regression coefficients.

Surface parameter	Linear equation	R²
$\varepsilon_s^d = d\gamma_s^d/dT$ (mJ m⁻² K⁻¹)	ε_s^d = -0.0454 % 5-FU - 0.4878	0.9292
$\gamma_s^d(T=0K)$ (mJ/m²)	$\gamma_s^d(T=0K)$ = 21.755 % 5-FU + 285.87	0.9341
T_{Max} (K)	T_{Max} = -5.241 % 5-FU + 583.49	0.8172

Table 1 clearly showed the important role of the modifier percentage on the various surface parameters of S-DVB copolymer.

Ou new results were compared to the those obtained by using the Dorris-Gray method [69]. This method used Equation (11) to determine γ_s^d of a solid material:

$$\gamma_s^d = \frac{\left[RTln\left[\frac{V_n\left(C_{n+1}H_{2(n+2)}\right)}{V_n\left(C_nH_{2(n+1)}\right)}\right]\right]^2}{4\mathcal{N}^2\, a^2_{-CH2-}\,\gamma_{-CH2-}} \tag{11}$$

where $C_nH_{2(n+1)}$ and $C_nH_{2(n+1)}$ are the respective formula of two consecutive n-alkanes, $a_{-CH2-}$the surface area of methylene group equal to 6 Å², and γ_{-CH2-} its surface energy.

The results obtained using Equation (11) were given in Table 3.

Table 3. Surface parameters of S-DVB copolymers using the Dorris-Gray method.

Copolymer	**$\gamma_s^d(T)$ (mJ/m²)**	**R²**	**$\varepsilon_s^d = d\gamma_s^d/dT$ (mJ m⁻² K⁻¹)**	**$\gamma_s^d(T=0K)$ (mJ/m²)**	**T_{Max} (K)**
S-DVB	$\gamma_s^d(T)$ = -3.048 T + 1515	0.9986	-3.048	1515.0	497.1
1% 5-FU / S-DVB	$\gamma_s^d(T)$ = -0.107 T + 145.05	0.9276	-0.107	145.1	1351.8
5% 5-FU / S-DVB	$\gamma_s^d(T)$ = 0.337 T - 50.531	0.986	0.337	-50.5	149.9
10% 5-FU / S-DVB	$\gamma_s^d(T)$ = 0.826 T - 266.14	0.9947	0.826	-266.1	322.1

Table 3 showed that the various surface parameters of the modified copolymers are very different from those obtained by our methodology. The deviation between the two methods results from the wrong hypothesis admitted by Dorris-Gray method supposing that the surface area of methylene group does not depend on the temperature. This hypothesis was proved by the Hamieh thermal to be wrong. Indeed, the Hamieh model took into account the effect of the temperature on the surface area of n-alkanes and polar solvents and consequently on the surface area of the methylene group.

3.3. Polar Free Energy of Adsorption

The values of $\left[-\Delta G_a^p(T)\right]$ of the adsorbed polar solvents were given in Table S1 versus the temperature. The evolution of $\left[-\Delta G_a^p(T)\right]$ against the temperature was drawn in Figure 3. The straight-lines plotted in Figure 3 led to the values of polar enthalpy $(-\Delta H_a^p)$ and entropy $(-\Delta S_a^p)$ of adsorption. The obtained results (Figure 3) proved that the solvents with the highest polarity such as i-butanol and i-propanol gave the highest polar free energy of adsorption whatever the used solid surface and for all temperatures. Whereas the lower polar free energy was obtained in the case of benzene and toluene due to their weaker polarity. Nevertheless, it was shown that when the 5-Fu percentage increased the polar free energy increased too and for all polar solvents (Figure 3).

The effect of the 5-FU percentage on the polar energy of adsorption was shown in Figure 4 for the different adsorbed solvents and at various temperatures.

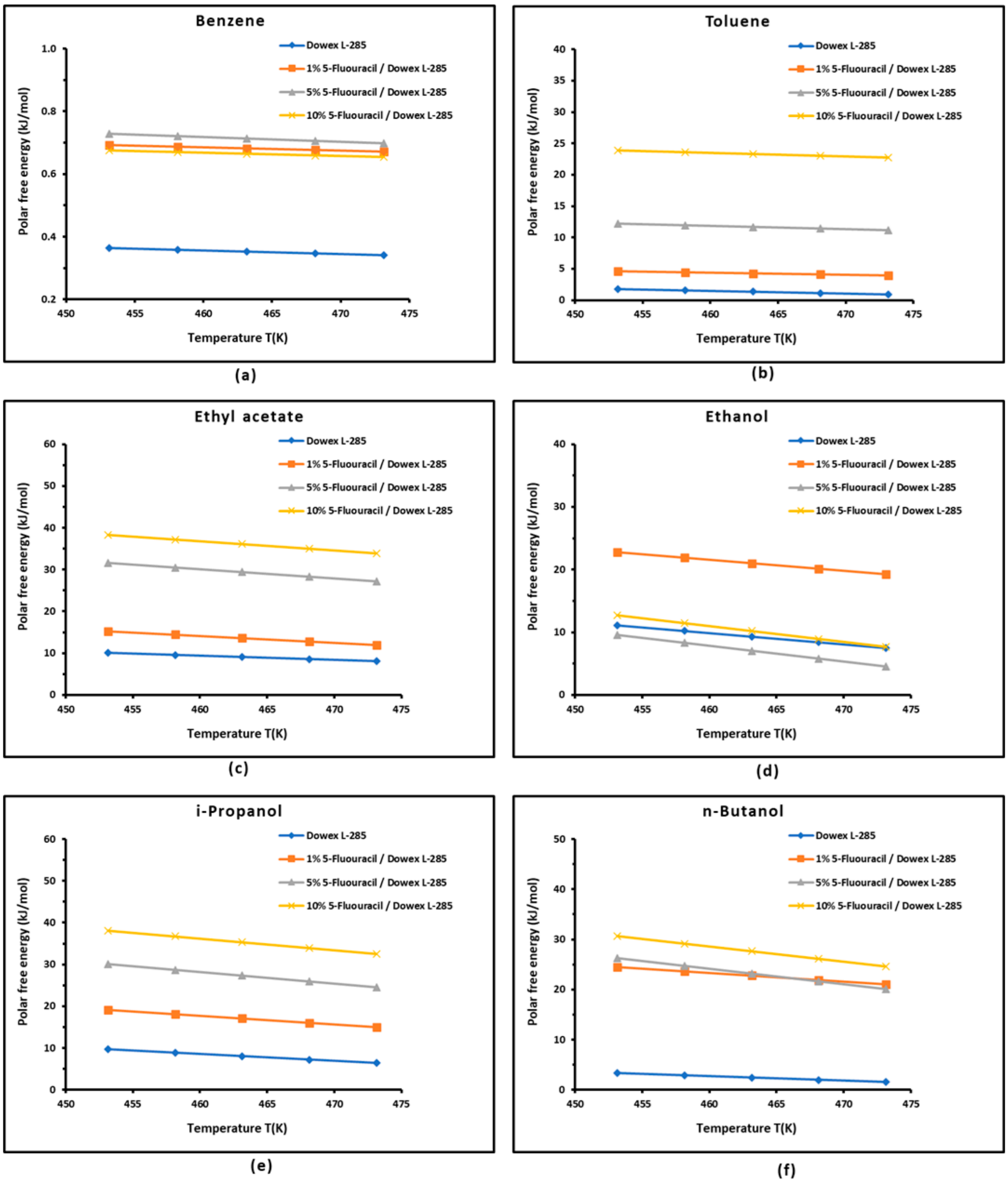
Benzene
Toluene
Ethyl acetate
Ethanol
i-Propanol
n-Butanol
Polar free energy (kJ/mol)
Temperature T(K)
Dowex L-285
1% 5-Fluouracil / Dowex L-285
5% 5-Fluouracil / Dowex L-285
10% 5-Fluouracil / Dowex L-285
450
455
460
465
470
475
0.2
0.4
0.6
0.8
1.0
0
5
10
15
20
25
30
35
40
50
60

(a) (b)

(c) (d)

(e) (f)

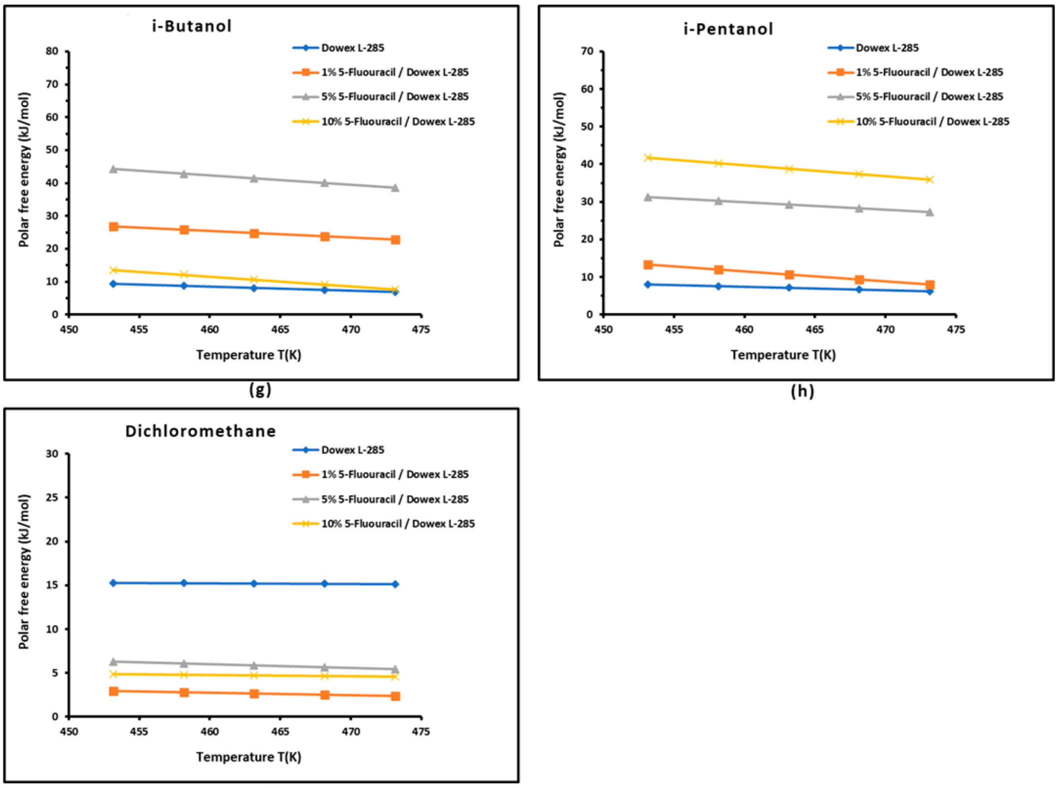

(g)

(h)

(i)

Figure 3. Evolution of the free polar energy $\left[-\Delta G_a^p(T)\right]$ of the various polar organic probes adsorbed on the different solid materials as a function of temperature for different 5-fluouracil percentages. (a) Benzene, (b) toluene, (c) ethyl acetate, (d) ethanol, (e) *i*-propanol, (f) *n*-butanol, (g) *i*-butanol, (h) i-pentanol, and (i) dichloromethane.

Different behaviors of the adsorbed polar probes were shown in Figure 4. A global increase of $\left[-\Delta G_a^p(T)\right]$ in the case of adsorption of solvents such as benzene, toluene, ethyl acetate, i-propanol, n-butanol, and i-propanol highlighting the strong effect of the modifier on the surface properties of the copolymer. An increase of $\left[-\Delta G_a^p(T)\right]$ was observed for ethanol followed by a sharp decrease after 1% 5-FU and stability after 5% 5-FU. Whereas a constant pallier was shown with n-butanol and dichloromethane after 1% 5-FU, while a maximum of $\left[-\Delta G_a^p(T)\right]$ was observed in the case of i-butanol, thus proving the important role of the terminal polar group of the adsorbed solvents on the modified S-DVB copolymer.

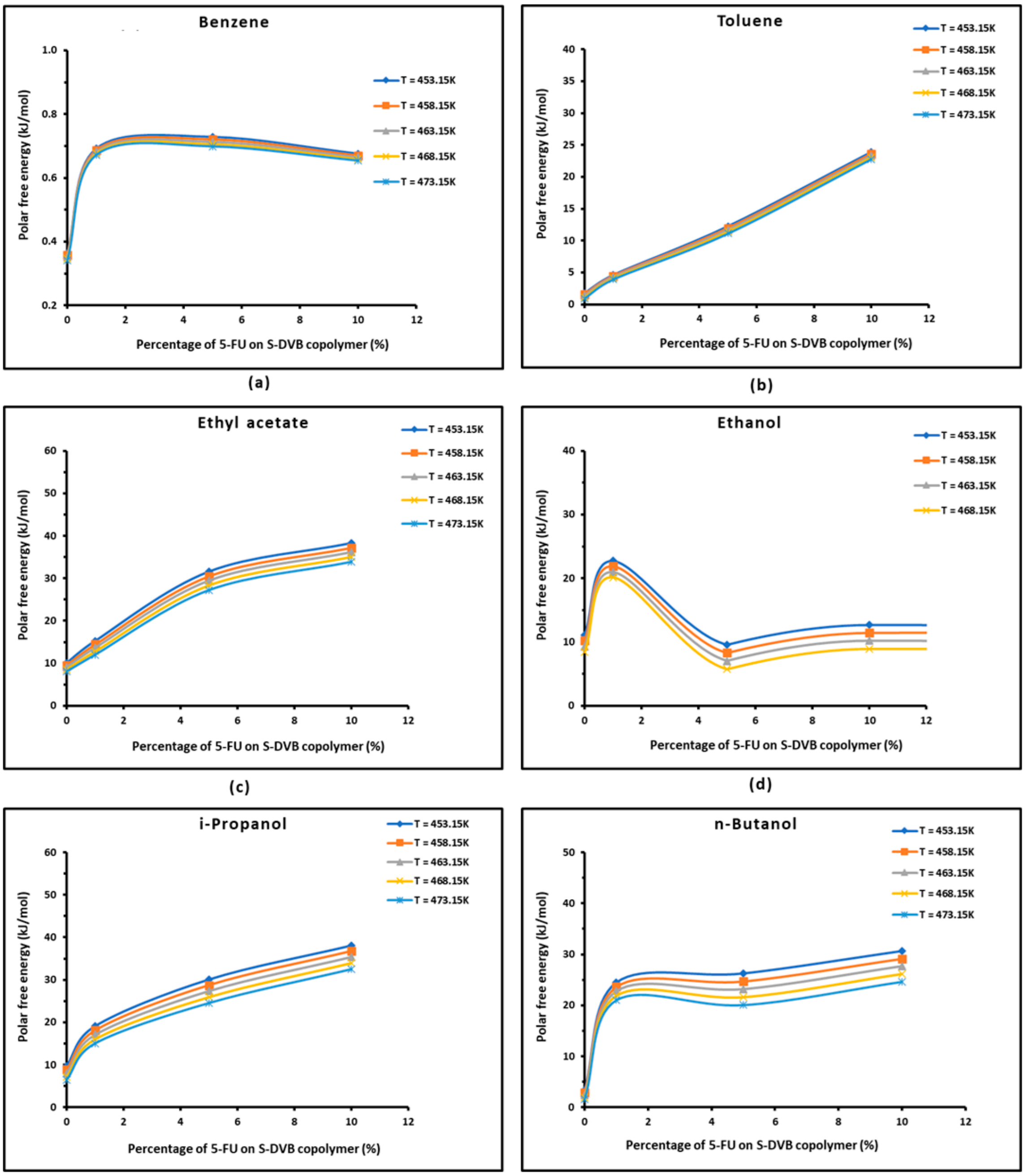
Benzene
Polar free energy (kJ/mol)
1.0
0.8
0.6
0.4
0.2
0
2
4
6
8
10
12
Percentage of 5-FU on S-DVB copolymer (%)
T = 453.15K
T = 458.15K
T = 463.15K
T = 468.15K
T = 473.15K
Toluene
40
35
30
25
20
15
10
5
Ethyl acetate
60
50
Ethanol
i-Propanol
n-Butanol

(a)

(b)

(c)

(d)

(e)

(f)

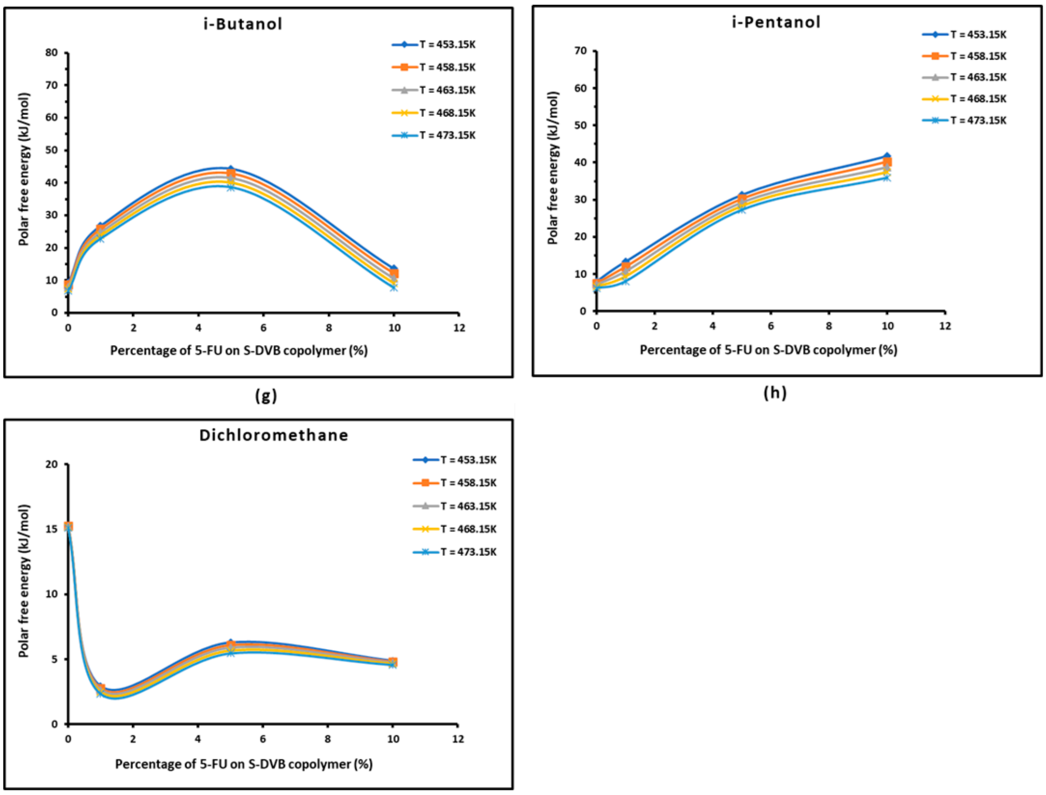

(g) (h)

(i)

Figure 4. Variations of $\left[-\Delta G_a^p(T)\right]$ of polar organic solvents versus the 5-fluouracil percentage for different temperature. (a) Benzene, (b) toluene, (c) ethyl acetate, (d) ethanol, (e) *i*-propanol, (f) *n*-butanol, (g) *i*-butanol, (h) i-pentanol, and (i) dichloromethane.

3.4. Lewis Acid–Base Properties

The values of the polar enthalpy $(-\Delta H_a^p)$ and entropy $(-\Delta S_a^p)$ of adsorption for the different copolymers obtained from the variations of $\left[-\Delta G_a^p(T)\right]$ of the adsorbed solvents given in Table S1 led deducing the Lewis acid-base parameters such as K_A, K_D, ω_A, and ω_D of the different copolymers. The results were then quantified by drawing in Figure 5 the evolution of $\left(\frac{-\Delta H_a^p}{AN'}\right)$ and $\left(\frac{-\Delta S_a^p}{AN'}\right)$ as a function of $\left(\frac{DN'}{AN'}\right)$ by varying the 5-FU percentage.

It was shown in Table 4. The results proved the amphoteric character of the different copolymers. A stronger Lewis acidity than the Lewis basicity was observed in the case of the S-DVB copolymer and for a modifier percentage equal to 1%. However, this tendency was inversed for a 5-FU percentage higher than 3% where the Lewis basicity was shown to be two times higher than their Lewis acidity.

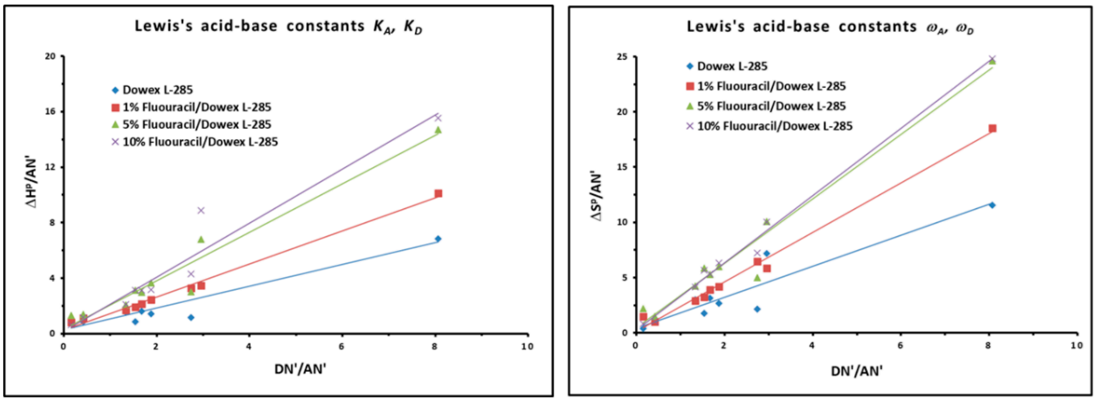

(a) (b)

Figure 5. Variations in $\left(\frac{-\Delta H_a^p}{AN'}\right)$ and $\left(\frac{-\Delta S_a^p}{AN'}\right)$ against $\left(\frac{DN'}{AN'}\right)$ of polar solvents adsorbed on the copolymer modified by different percentages of 5-FU.

Table 4. Values of the Lewis acid–base constants K_A, K_D, ω_A, and ω_D; and the acid–base ratios of the different modified copolymers with the global acid-base parameters $S_K = K_A + K_D$ and $S'_K = \omega_A + \omega_D$ with the linear regression coefficient R^2.

Material	K_D	K_A	K_D/K_A	$K_A + K_D$	R²	$10^{-3}\omega_D$	$10^{-3}\omega_A$	ω_D/ω_A	$10^{-3}(\omega_A + \omega_D)$	R²
Dowex-L-285	0.283	0.786	0.36	1.07	0.886	0.43	1.41	0.30	1.83	0.871
1% 5-FU on S-DVB-L-285	0.261	1.193	0.22	1.45	0.9909	0.12	2.24	0.06	2.37	0.990
5% 5-FU on S-DVB-L-285	0.31	1.750	0.18	2.06	0.950	0.67	2.87	0.23	3.55	0.9575
10% 5-FU on S-DVB-L-285	0.177	1.950	0.09	2.13	0.937	0.24	3.05	0.08	3.29	0.9921

All solid surfaces exhibited an amphoteric character (Table 4) showing higher Lewis acidity reaching $K_A = 1.95$, with a decrease of the Lewis basicity force from $K_D = 0.283$ for S-DVB copolymer to $K_D = 0.177$ in the case 10% 5-FU on the S-DVB copolymer. An increase of the Lewis acidity was observed when the 5-FU percentage increased. The Lewis acidity of the modified copolymer increased 2.48 times with 10% 5-FU, while its basicity decreased 0.63 time relative to the alone copolymer. However, the global acid-base character given by S_K and S'_K strongly increased with the increase of the 5-FU percentage. These important results confer to the S-DVB modified by 5-FU to be an excellent candidate in several pharmaceutical and industrial applications that require more Lewis acid-base character.

The study of the various Lewis acid-base parameters against the 5-FU percentage led to the linear equations presented in Table 5 and plotted in Figure 6. Even if the linear regression coefficients are moderately acceptable, however, the different linear relations in Table 5 and shown in Figure 6 proved the crucial role of the addition of 5-FU in the S-DVB copolymer and the increase of the surface groups in the modified copolymer.

Table 5. Equations of Lewis acid-base parameters as a function of %5-FU with the corresponding linear regression coefficients.

Parameter	Equation	R²
K_A	K_A = 0.109 % 5-FU + 0.986	0.8804
K_D	K_D = -0.009 % 5-FU + 0.293	0.8655
K_D/K_A	K_D/K_A = -0.022 % 5-FU + 0.300	0.8048
$S_K = K_D + K_A$	S_K=0.100 % 5-FU + 1.279	0.8025
ω_A	ω_A = 0.142 % 5-FU + 1.824	0.7003
ω_D	ω_D = 0.001 % 5-FU + 0.363	0.7541
ω_D/ω_A	ω_D/ω_A = -0.011 % 5-FU + 0.211	0.7647
$S'_K = \omega_D + \omega_A$	S_K = 0.143 %5-FU + 2.187	0.8592

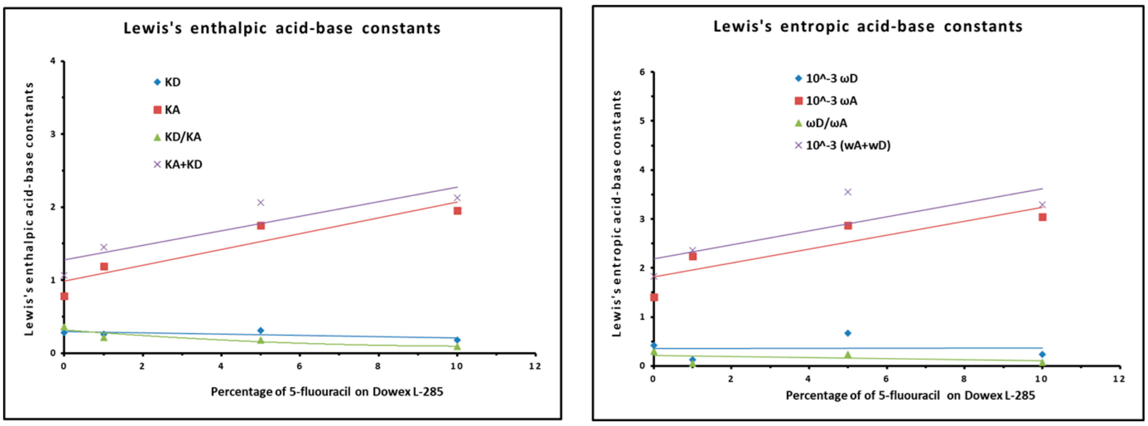

(a) (b)

Figure 6. Variations of the Lewis acid-base parameters versus 5-FU percentage.

3.5. Polar surface energies

The values of $-\Delta G_a^p(T)$ of dichloromethane and ethyl acetate given in Table 6 led to those of the polar acid $\gamma_s^+(T)$ and base $\gamma_s^-(T)$ surface energies of the modified S-DVB copolymer, and therefore to the values of the polar surface energy $\gamma_s^p(T)$ as well as the total surface energy $\gamma_s^{tot.}(T)$ of the solid surfaces .The variations of the various surface energies were plotted in Figure 7.

Table 6. Values of $-\Delta G_a^p(T)$ (in kJ/mol) of dichloromethane and ethyl acetate adsorbed on the modified copolymer for various temperatures.

Dichloromethane				
T(K)	S-DVB copolymer	1% 5-FU/S-DVB	1% 5-FU/S-DVB	10% 5-FU/S-DVB
453.15	15.274	2.922	6.291	4.884
458.15	15.239	2.783	6.087	4.809
463.15	15.204	2.643	5.882	4.734
468.15	15.169	2.504	5.678	4.659
473.15	15.134	2.364	5.473	4.584
Ethyl Acetate				
T(K)	S-DVB copolymer	1% 5-FU/S-DVB	1% 5-FU/S-DVB	10% 5-FU/S-DVB
453.15	10.106	15.293	31.618	38.307
458.15	9.593	14.470	30.525	37.207
463.15	9.079	13.646	29.433	36.107
468.15	8.566	12.823	28.340	35.007
473.15	8.052	11.999	27.248	33.907

The straight-lines representing the evolution of different surface energy parameters plotted in Figure 7 showed large difference depending on the 5-FU percentage, the temperature and the surface energy type. A maximum of the surface energy was obtained for the highest 5-FU percentage (10%). All surface energy parameters presented a decrease versus the temperature.

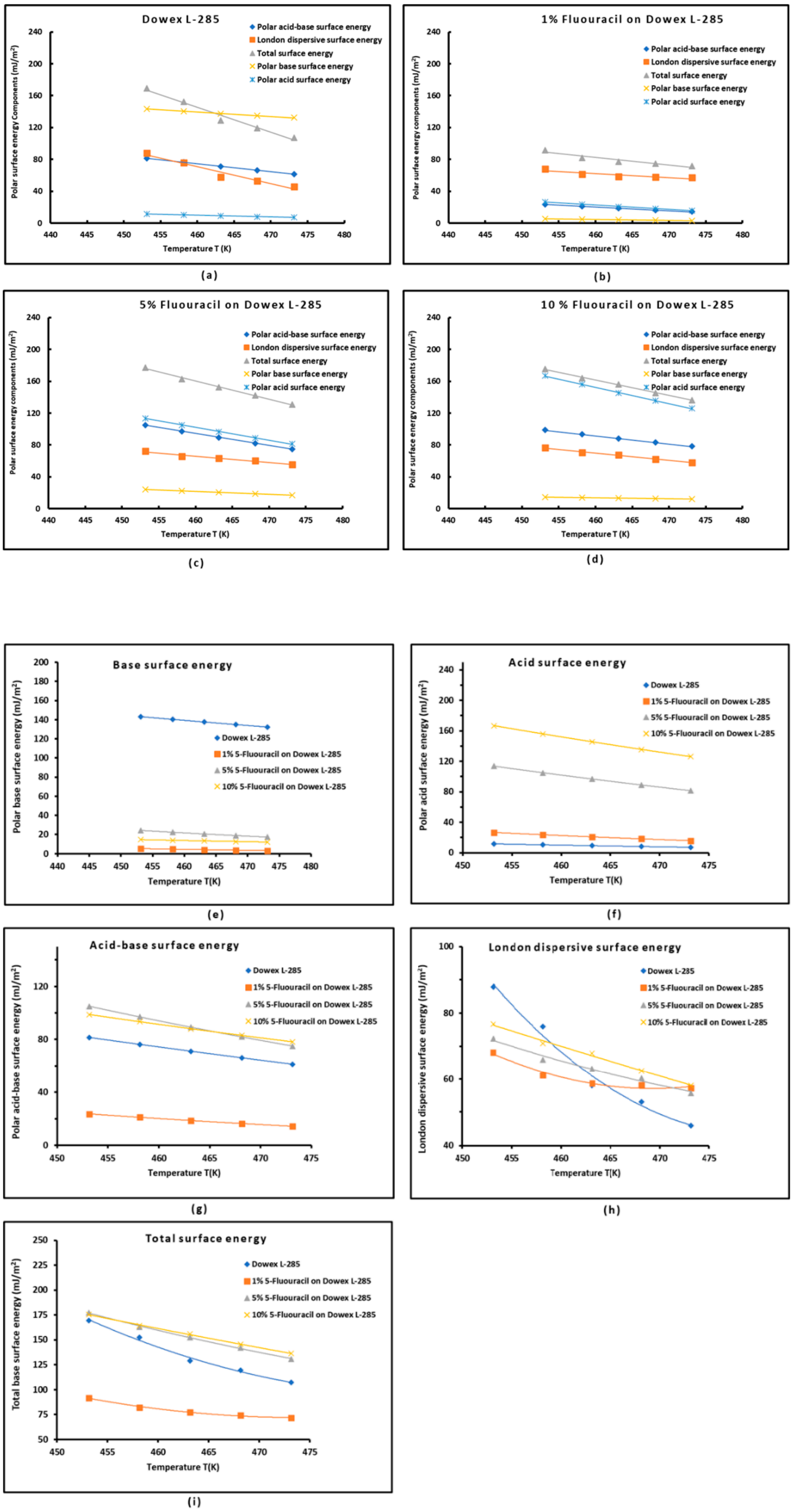

(a) (b) (c) (d) (e) (f) (g) (h) (i)

Figure 7. Variations of the different surface energy components of the modified S-DVB copolymer versus the temperature: Dowex L-285 copolymer (a), 1% 5-FU (b), 5% 5-FU (c), 10% 5-FU (d), base surface energy (e), acid

surface energy (f), acid–base surface energy (g), London dispersive surface energy (h), and total surface energy (i).

Our new methodology applied to the various copolymers led to the values of the polar surface energy of the solvents drawn in Figure 8, for the different 5-FU percentages. Results in Figure 8 showed that the polar surface energy of the solvents was the lowest in the case of adsorption on S-DVB copolymer (Dowex L-285), while the highest values were obtained in the case of 10% 5-FU on S-DVB copolymer. The conclusions observed in the section are the same as those obtained in other studies [28,29] carried out with other modifiers.

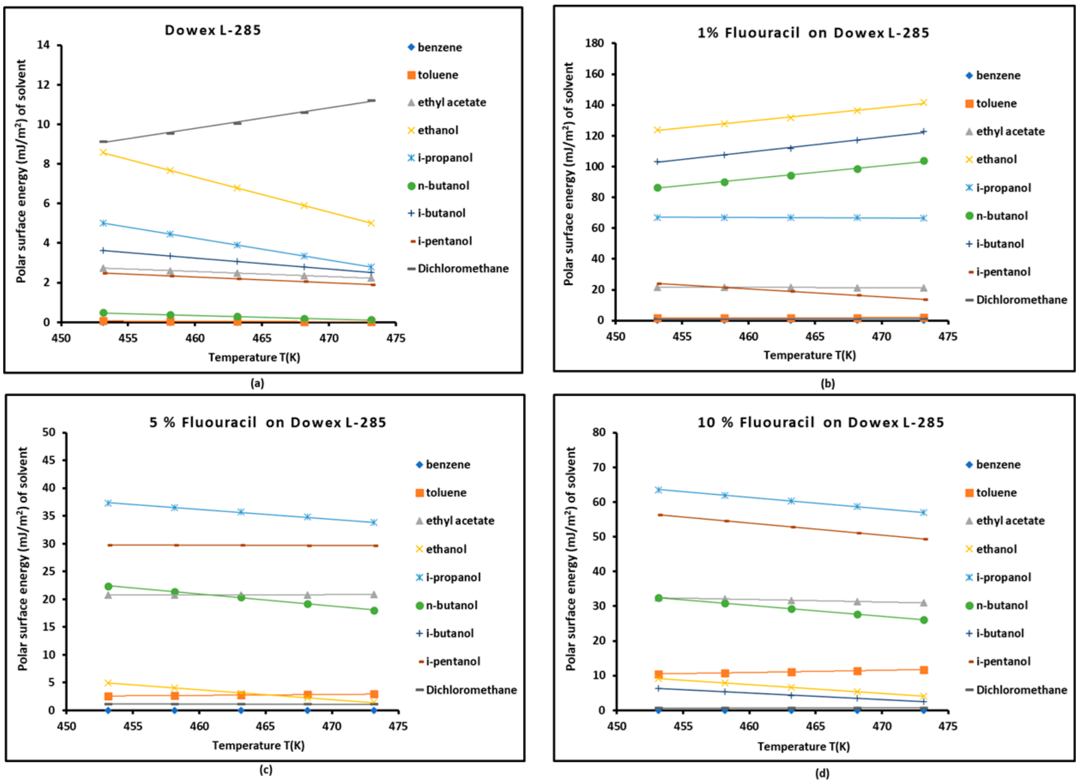

(a) (b) (c) (d)

Figure 8. Variations in polar surface energy (in mJ/m^2) of the different polar solvents adsorbed on Dowex L-285 modified by varying the 5-FU percentage as a function of temperature: Dowex L-285 (a), 1% 5-FU (b), 5% 5-FU (c), and 10% 5-FU (d).

3.6. Determination of the Average Separation Distance H

Previous results led to the determination of the separation distance H between the solvent and the S-DVB modified by 5-FU at various temperatures. The obtained results given in Figure 9 highlighted a difference in the variations of $H(T)$ between the different solid surfaces, where a slight decrease was observed for the various 5-FU percentages when the temperature increased, whereas an increase of $H(T)$ was noticed with S-DVB copolymer

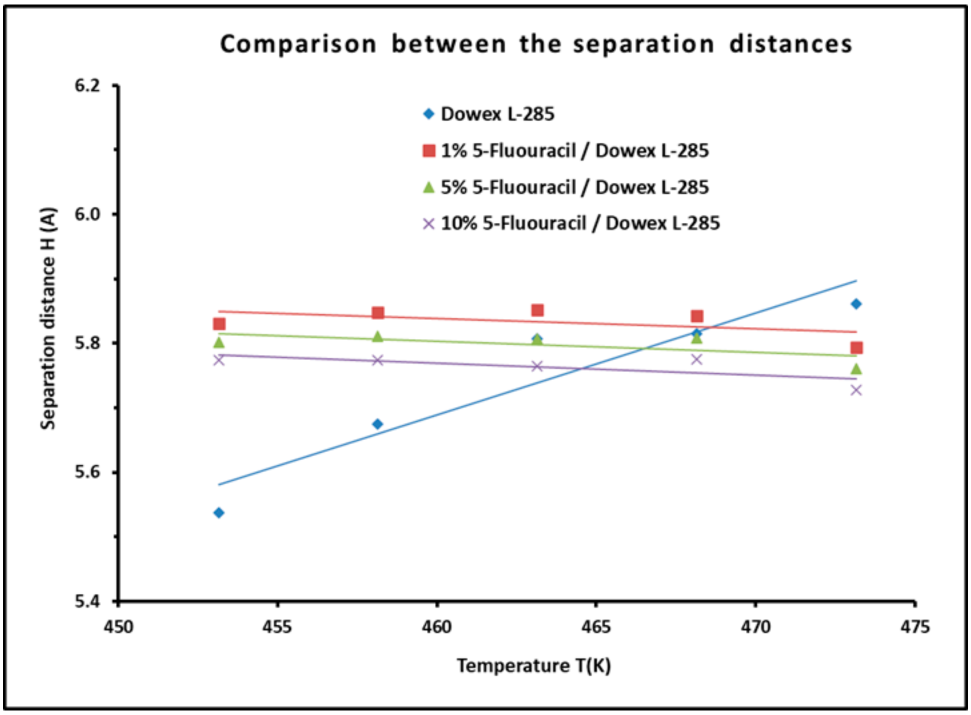

Figure 9. Evolution of the separation distance $H(T)$ (in Å) for the modified copolymers versus the temperature.

3.7. Comparison with Previous Works and Discussion

The present study was devoted to the determination of the surface properties of the styrene–divinylbenzene copolymer modified by 5-fluouracil at different percentages from 1% to 10%, while the previous studies [28,29] were interested in studying the same copolymer but with other modifiers such as melamine [28] and 5-hydroxy-6-methyluracil [29].

Considering the results of the London dispersive surface energy obtained with 1% of the modifier on S-DVB, it was possible to study the effect of the modifier on $\gamma_s^d(T)$ of the modified copolymer. The different equations of $\gamma_s^d(T)$ were presented in Table 7 and their variations plotted in Figure 10.

Table 7. Comparison between $\gamma_s^d(T)$ of the modified S-DVB copolymer.

Modified copolymer	$\gamma_s^d(T)$ (mJ/m²)	R²	$\varepsilon_s^d = d\gamma_s^d/dT$ (mJ m⁻² K⁻¹)	$\gamma_s^d(T=0K)$ (mJ/m²)	$\gamma_s^d(T=298.15K)$ (mJ/m²)	T_{Max} (K)
1% Melamine/S-DVB	$\gamma_s^d(T)$= -0.907T + 496.21	0.9972	-0.907	496.21	225.79	547.1
1% HMU/S-DVB	$\gamma_s^d(T)$ = -0.874T + 444.68	0.9837	-0.874	444.68	184.16	508.9
1% 5-FU/S-DVB	$\gamma_s^d(T)$ = -0.497T + 290.95	0.8900	-0.497	290.95	142.77	585.4

Table 7 showed that the surface entropy decreased in absolute value as follows:

1% Melamine/S-DVB > 1% HMU/S-DVB > 1% 5-FU/S-DVB

The extrapolated London dispersive surface energy at 0K decreased from melamine to 5-fluouracil. However, the lowest maximum temperature was obtained with 1% 5-hydroxy-6-methyluracil. Whereas, Figure 10 allowed classifying the $\gamma_s^d(T)$ of the various modifiers in decreasing order as follows:

1% Melamine/S-DVB > 1% 5-FU/S-DVB > 1% HMU/S-DVB

The results in Figure 10 highlighted a highest $\gamma_s^d(T)$ with melamine on S-DVB copolymer was obtained, probably due to the severe modification in the surface groups of S-DVB modified by the supramolecule structure of melamine.

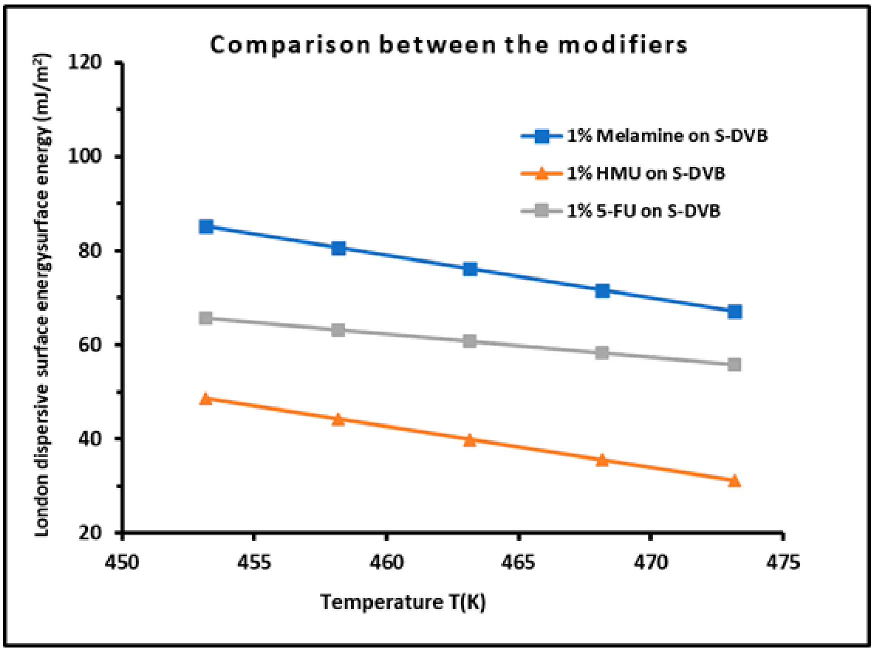

Figure 10. Comparison between the London dispersive surface energy of S-DVB copolymer modified by 1% of the different modifiers.

The comparison between the polar free energy of the various polar solvents adsorbed on the different modified copolymers allowed drawing the curves of Figure 11 that clearly showed the lowest values of $-\Delta G_a^p(T)$ in the case of S-DVB modified by melamine proving the lowest surface groups present at the surface of the modified copolymer. It was observed in Figure 11 that 5-fluouracil on S-DVB gave the highest polar free energy for most polar organic solvents, except for ethyl acetate and toluene that exhibited the highest $-\Delta G_a^p(T)$ with S-DVB modified by 5-hydroxy-6-methyluracil.

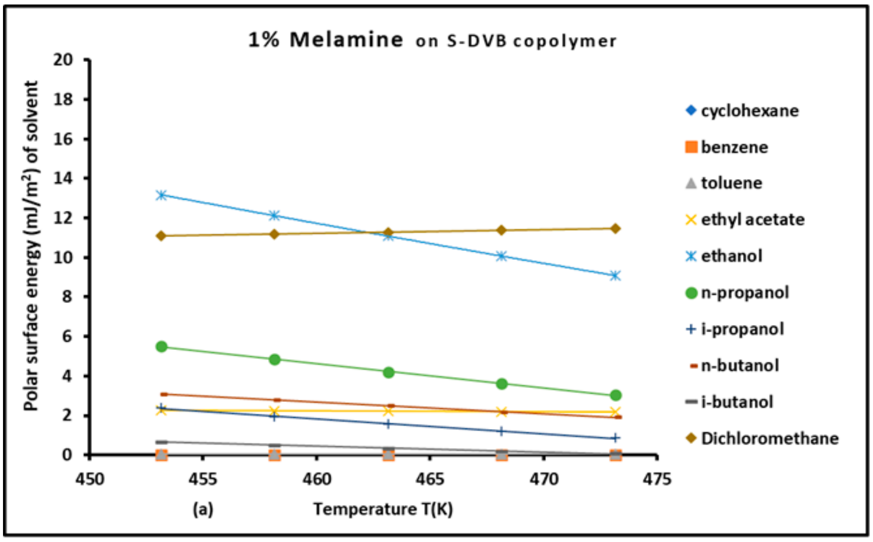

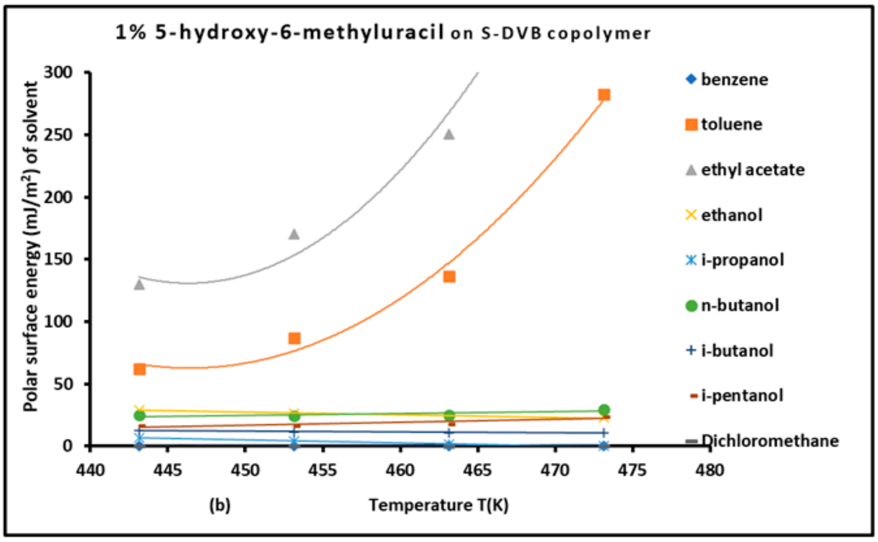

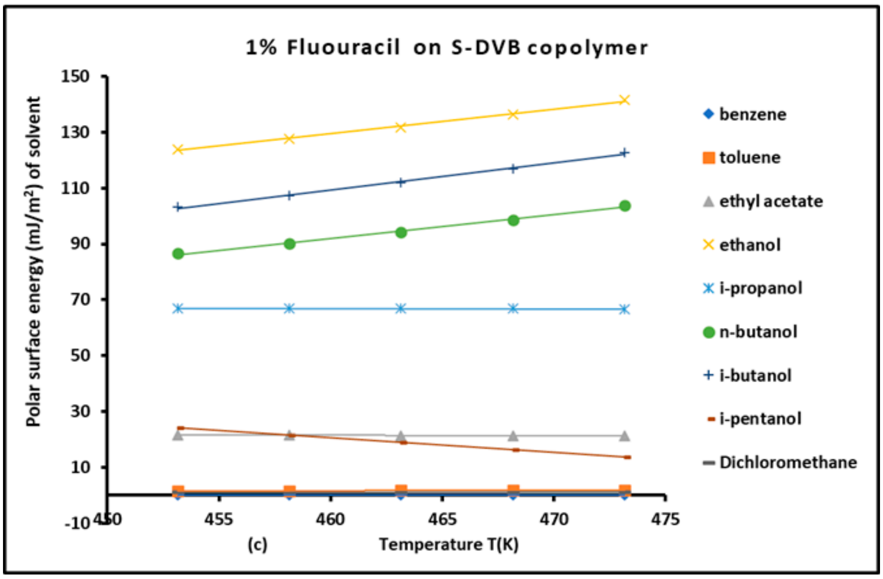

Figure 11. comparison between the free polar energy $\left[-\Delta G_a^p(T)\right]$ of polar organic probes adsorbed on the different copolymers modified by melamine (a), 5-hydroxy-6-methyluracil, and 5-flouuracil versus the temperature.

In order to better understand the effect of the various modifiers on the Lewis acid-base properties, we gave in Figure 12 the structure of these molecules as well their acid-base character.

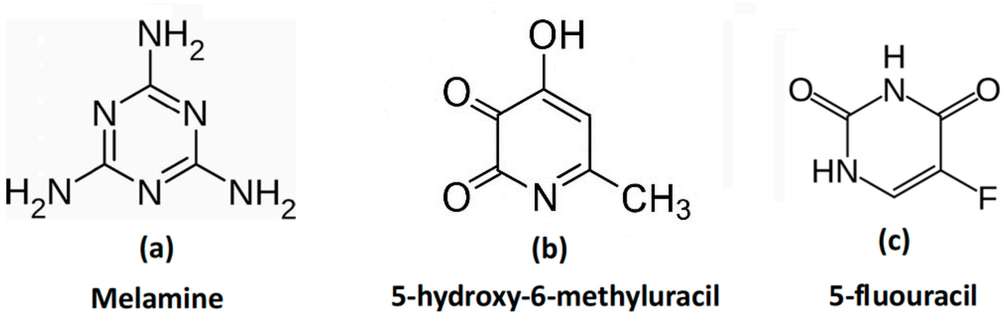

(a)
Melamine

(b)
5-hydroxy-6-methyluracil

(c)
5-fluouracil

Figure 12. Planar structure of the different modifiers: melamine (a), 5-hydroxy-6-methyluracil (b), and 5-fluouracil (c).

The first modifier used in the first work [28] is the melamine that can be considered as a strong Lewis Base. Indeed, each –NH_2 group in his structure has a lone pair on the nitrogen, making them electron-rich (Figure 12a). The nitrogen atoms in the triazine ring also contain lone pairs (though their availability is reduced due to aromatic delocalization). Therefore, melamine can donate lone pairs, especially via its amino groups, to Lewis acids. Melamine is not a Lewis acid because it cannot accept electrons.

The second modifier, the 5-hydroxy-6-methyluracil molecule [29], is a pyrimidine derivative and includes the following key groups: two carbonyl groups (=O) at positions 2 and 4 (like in uracil), a hydroxy group (–OH) at position 5, a methyl group (–CH_3) at position 6 and nitrogen atoms at positions 1 and 3 (part of the ring) (Figure 12b). The carbonyl oxygen atoms (at positions 2 and 4) have lone pairs that can donate electrons and give Lewis base sites. Whereas, the hydroxy group at position 5 also has a lone pair on oxygen and can also act as a Lewis base. While the Ring nitrogen atoms have lone pairs, and depending on tautomeric form and protonation state, they may participate as electron donors. This makes 5-hydroxy-6-methyluracil molecule as Lewis base, because it has multiple Lewis base sites, thanks to its oxygen and nitrogen atoms with lone pairs. On the other hand, the hydrogen atoms on the –OH or ring NH groups can participate in hydrogen bonding, but that's Bronsted acidity, not strictly Lewis acidity. This molecule then lacks empty orbitals or strongly electron-deficient centers and cannot be a Lewis acid.

Finally, the 5-fluorouracil (5-FU) contains base ring (Figure 12c): pyrimidine with six-membered ring with nitrogen atoms (at positions 1 and 3) presenting lone pairs that can interact with acid sites, carbonyl groups (=O) at positions 2 and 4 that can donate electrons, and a fluorine atom at position 5, strongly electronegative, having lone pairs, though less available for bonding due to strong bond to carbon. 5-FU is then a Lewis base, capable of donating electron pairs, especially through its carbonyl oxygens and ring nitrogen atoms.5-FU cannot easily interact as Lewis acid because it does not readily accept electron pairs. In conclusion, the three modifiers can be classified in increasing order of Lewis basicity as follows:

5-Fluorouracil < 5-Hydroxy-6-methyluracil < Melamine

The Lewis acid-base results obtained with the three modifiers are given in Table 8. It can be observed that the S-DVB modified by melamine exhibited the highest Lewis acidity relatively to the other modifiers, followed by the copolymer modified by 5-fluouracil and the lowest Lewis acidity was obtained with the modification by 5-Hydroxy-6-methyluracil. Whereas the highest Lewis basicity was obtained with 5-Hydroxy-6-methyluracil followed respectively by 5-fluouracil and melamine modifiers. These results are in good agreement with the Lewis acid-base character discussed above. Indeed, the highest basicity of melamine after addition to S-DVB copolymer, conferred to the modified copolymer the highest acidity relatively to the two other modifiers.

However, the highest basicity of the copolymer modified by 5-hydroxy-6-methyluracil is certainly due to the presence of three oxygen atoms which enhance the Lewis basic character of the modified copolymer.

Table 8. Comparison between the Lewis's acid-base parameters of the modified copolymer for the various modifiers (at 1%).

Modified copolymer	K_A	K_D	K_A/K_D	K_A+K_D	R²	$10^{-3}\omega_A$	$10^{-3}\omega_D$	ω_A/ω_D	$10^{-3}(\omega_A+\omega_D)$	R²
1% Melamine/S-DVB	1.455	0.164	8.85	1.620	0.9783	0.09	2.81	0.03	2.90	0.9316
1% HMU/S-DVB	0.459	0.696	1.52	1.155	0.9561	0.81	1.64	0.49	2.45	0.975
1% 5-FU/S-DVB	1.193	0.261	4.57	1.45	0.9909	2.24	0.12	2.37	18.1	0.9904

4. Conclusions

All surface thermodynamic parameters of the styrene–divinylbenzene copolymer modified by 5-fluouracil were determined by varying the modifier percentage (from 1% to 10%) and for various temperatures. The free energy of adsorption of model organic molecules was obtained using the IGC technique at infinite dilution, the Hamieh thermal model, and the new method of the separation of the dispersive and polar components of the polar molecules adsorbed on the modified S-DVB copolymer. The new results proved that the highest energy of adsorption was obtained with the modified S-DVB for the highest percentage of 5-FU, and the highest free energy was obtained with i-butanol and i-propanol. Whereas, the London dispersive surface energy of S-DVB copolymer decreased by adding the modifier 5-FU for a percentage of 1%. The comparison between the Hamieh thermal model and the Dorris-Gray method showed an important deviation between the two methods due to the wrong hypothesis admitted by Dorris-Gray method supposing that the surface area of methylene group does not depend on the temperature. It was also observed that the solvents with the highest polarity such as i-butanol and i-propanol gave the highest polar free energy of adsorption whatever the used solid surface and for all temperatures. Whereas, the lower polar free energy was obtained in the case of benzene and toluene due to their weaker polarity, while the polar free energy increased for all polar solvents when the 5-Fu percentage increased. An amphoteric character of the different copolymers was showed. A higher Lewis acidity of the S-DVB copolymer was observed in the case of a modifier percentage equal to 1%. It was proved that the polar surface energy of the solvents was the lowest in the case of adsorption on alone S-DVB copolymer, while the highest values were obtained in the case of 10% 5-FU on S-DVB copolymer. The comparison between the different modifiers led us classifying their $\gamma_s^d(T)$ in decreasing order as follows:

1% Melamine/S-DVB > 1% 5-FU/S-DVB > 1% HMU/S-DVB

This highlighted a highest $\gamma_s^d(T)$ with melamine on S-DVB copolymer, probably due to the severe modification in the surface groups of S-DVB modified by the supramolecule structure of melamine. Furthermore, the lowest values of $-\Delta G_a^p(T)$ was obtained in the case of S-DVB modified by melamine proving the lowest surface groups of the modified copolymer. It was showed that 5-fluouracil on S-DVB gave the highest polar free energy for most polar organic solvents, except for ethyl acetate and toluene that exhibited the highest $-\Delta G_a^p(T)$ with S-DVB modified by 5-hydroxy-6-methyluracil. It can be also noticed that the S-DVB modified by melamine exhibited the highest Lewis acidity relatively to the other modifiers, followed by the copolymer modified by 5-fluouracil and the lowest Lewis acidity was obtained with the modification by 5-Hydroxy-6-methyluracil. Whereas the highest Lewis basicity was obtained with 5-Hydroxy-6-methyluracil followed respectively by 5-fluouracil and melamine modifiers.

Supplementary Materials: Table S1. Variations in $\Delta G_a^p(T)$ (kJ/mol) of different polar solvents adsorbed on Dowex L-285 and various 5-fluouracil percentages as a function of temperature. Table S2. Values of $\gamma_s^+(T)$, $\gamma_s^-(T)$, $\gamma_s^{AB}(T)$, γ_s^d (T), and $\gamma_s^{tot.}(T)$ of Dowex L-285 and the different percentages of 5-fluouracil on the copolymer.

Author Contributions: Conceptualization, T.H. and V.Y.G.; methodology, T.H.; software, T.H.; validation, T.H. and V.Y.G.; formal analysis, T.H. and V.Y.G.; investigation, T.H. and V.Y.G.; resources, V.Y.G.; data curation,

V.Y.G.; writing—original draft preparation, T.H.; writing—review and editing, T.H.; visualization, T.H. and V.Y.G.; project administration, T.H. and V.Y.G.; funding acquisition, V.Y.G. All authors have read and agreed to the published version of the manuscript.

Funding: This research received no external funding.

Informed Consent Statement: Not applicable.

Institutional Review Board Statement: Not applicable.

Data Availability Statement: The data presented in this study are available in the article and Supplementary Materials.

Conflicts of Interest: The authors declare no conflicts of interest.

References

1. De Oliveira Reis, M.; de Sousa, R.G.; de Souza Medeiros Batista, A. Synthesis and characterization of poly(styrene-co-divinylbenzene) and nanomagnetite structures, *Methods X*, **2022**, *9*, 2022, 101764, https://doi.org/10.1016/j.mex.2022.101764.
2. Ramos, G.S.M.; Mendes, M.S.L.; Neves, M.A.F.S.; Pedrosa, M.S.; Silva, M.R. Experimental design to evaluate the efficiency of maghemite nanoparticles incorporation in styrene-divinylbenzene copolymers, *J. Appl. Polym. Sci.* 2021, *138* (18), 50318.
3. Rodrigo, R.; Toro, C.A.; Cuellar, J. Morphological characteristics of poly(styrene-co-divinylbenzene) microparticles synthesized by suspension polymerization, Powder Technol. 247 (2013) 279–288.
4. Li, T.; Liu, H.; Zeng, L.; Yang, S.; Li, Z.; Zhang, J.; Zhou, Z. Macroporous magnetic poly(styrene–divinylbenzene) nanocomposites prepared via magnetite nanoparticles-stabilized high internal phase emulsions, *J. Mater. Chem*. **2011**, 21, 12865–12872.
5. Stuurman, H.W., Köhler, J., Jansson, S.O. *et al.* Characterization of some commercial poly (styrene-divinylbenzene) copolymers for reversed-phase HPLC[1] . *Chromatographia* **23**, 341–349 (1987). https://doi.org/10.1007/BF02316180.
6. da Cunha, L., Coutinho, F.M.B., Teixeira, V.G. *et al.* Surface modification of styrene-divinylbenzene copolymers by polyacrylamide grafting via gamma irradiation . *Polym. Bull.* **61**, 319–330 (2008). https://doi.org/10.1007/s00289-008-0962-2.
7. Valencia-Lazcano, A.A.; Hassan, D.; Pourmadadi, M.; shamsabadipour,A.; Behzadmehr, R.; Rahdar, A.; Medina, D.I.; Díez-Pascual,A.M. 5-Fluorouracil nano-delivery systems as a cutting-edge for cancer therapy, *European Journal of Medicinal Chemistry*, **2023**, 246, 114995, https://doi.org/10.1016/j.ejmech.2022.11499.
8. Abdullah, S.; El Hadad, S.; Aldahlawi A. The development of a novel oral 5-Fluorouracil in-situ gelling nanosuspension to potentiate the anticancer activity against colorectal cancer cells, *Int. J. Pharm*., **2022**, *613*, 121406. https://doi.org/10.1016/j.ijpharm.2021.121406.
9. Olukman, M.; Sanli, O.; Solak, E.K.; Release of Anticancer Drug 5-Fluorouracil from Different Ionically Crosslinked Alginate Beads. *J. Biomater. Nanobiotechnol*. **2012**, *03*, 469–479.
10. Ortiz, R.; Cabeza, L.; Arias, J.L.; Melguizo, C.; Alvarez, P.J.; Velez, C.; Clares, B.; Aranega, A.; Prados, J. 2015. Poly(butylcyanoacrylate) and Poly(epsilon- caprolactone) Nanoparticles Loaded with 5-Fluorouracil Increase the Cytotoxic Effect of the Drug in Experimental Colon Cancer. *AAPS J*. **2015**, *17*, 918–929.
11. Shishu, G. N.; Aggarwal, N. Stomach-specific drug delivery of 5-fluorouracil using floating alginate beads. *AAPS Pharm. Sci. Tech*. **2007**, *8*, E143–E149.
12. Siemiaszko, G.; Niemirowicz-Laskowska, K.; Markiewicz, K.H.; Dudź, E.; Milewska, S.; Misiak, P.; Kurowska, I.; Sadowska, A.; Car, H.; Wilczewsk, A.Z. Synergistic effect of folate-conjugated polymers and 5-fluorouracil in the treatment of colon cancer. *Cancer Nano* **12**, 31 (2021). https://doi.org/10.1186/s12645-021-00104-9.
13. Kopeček, J. Smart and genetically engineered biomaterials and drug delivery systems, *European Journal of Pharmaceutical Sciences*, **2003**, *20* (1), 1-16.
14. Singh P, Tyagi G, Mehrotra R, Bakhshi AK. Thermal stability studies of 5-fluorouracil using diffuse reflectance infrared spectroscopy. Drug Test Anal. 2009, 1(5), 240-244. https://doi.org/10.1002/dta.41.

15. Bergbreiter, D.E. Polymer-supported reagents and catalysts in organic synthesis, *Chemical Reviews*, **2002**, *102* (10), 3345-3384.
16. Parisi, E.; Garcia, A.M.; Marson, D.; Posocco, P.; Marchesan, S. Supramolecular Tripeptide Hydrogel Assembly with 5-Fluorouracil. Gels. 2019, 5(1), 5. https://doi.org/10.3390/gels5010005.
17. Pan, B.; Xing, B. Adsorption mechanisms of organic chemicals on carbon nanotubes, Environmental Science & Technology, 2008, 42 (24), 9005-9013.
18. Zhang, L.; Chen, X.; Zhang, H.; Zhang, H.; Guo, H.; Wang, C.; Wang, M.; Yao, S.; Lin; X.; Chen, X. Preparation of Polar-Modified Styrene-Divinylbenzene Copolymer and Its Adsorption Performance for Comprehensive Utilization of Sugarcane Bagasse Dilute-Acid Hydrolysate. *Appl Biochem Biotechnol* **190**, 423–436 (2020). https://doi.org/10.1007/s12010-019-03100-3
19. Vashurin, A. S.; Barabanov, V. M. Coordination and Sorption Capabilities of 5-fluouracil-Based Compounds. *Russ. J. Gen. Chem.* **2015**, *85*(10), 2287–2292.
20. Pałasz, A.; Cież, D. In search of uracil derivatives as bioactive agents. Uracils and fused uracils: Synthesis, biological activity and applications, *European Journal of Medicinal Chemistry*, **2015**, *97*, 582-611, https://doi.org/10.1016/j.ejmech.2014.10.008.
21. Samuilov, P. Modified uracils in medicinal chemistry. *Russian Chemical Reviews*, **2016**, 85(4), 374–390.
22. Epure, E.L.; Moleavin, I.A.; Taran, E. Nguyen, A.V.; Nichita, N.; Hurduc, N. Azo-polymers modified with nucleobases and their interactions with DNA molecules. *Polym. Bull.* **2011**, *67*, 467–478, https://doi.org/10.1007/s00289-010-0436-1.
23. Zaitsev, S.Yu.; Vereschetin, V.P.; Gromov, S.P.; Fedorova, O.A.; Alfimov, M.V.; Huesmann, H.; Möbius, D. Photosensitive supramolecular systems based on amphiphilic crown ethers, *Supramol. Sci.* **1997**, *4*, 519–524. https://doi.org/10.1016/S0968-5677(97)00037-0.
24. Gus'kov, V.Y.; Bilalova, R.V.; Kudasheva, F.K. Adsorption of organic molecules on a 5-fluouracil -modified porous polymer. *Russ. Chem. Bull.* **2017**, *66*, 857–861. https://doi.org/10.1007/s11172-017-1818-4.
25. Gainullina, Y.Y.; Gus'kov, V.Y.; Timofeeva, D.V. Polarity of Thymine and 6-Methyluracil-Modified Porous Polymers, According to Data from Inverse Gas Chromatography. *Russ. J. Phys. Chem.* **2019**, *93*, 2477–2481. https://doi.org/10.1134/S0036024419120082.
26. Gus'kov, V.Y.; Gainullina, Y.Y.; Ivanov, S.P.; Kudasheva; F.K. Thermodynamics of organic molecule adsorption on sorbents modified with 5-fluouracil by inverse gas chromatography. *Journal of chromatography. A*, **2014**, *1356*, 230-235.
27. Gus'kov, V.Y.; Ivanov, S.P.; Khabibullina, R.A.; Garafutdinov, R.R.; Kudasheva, F.K. Gas chromatographic investigation of the properties of a styrene-divinylbenzene copolymer modified by 5-fluouracil. *Russ. J. Phys. Chem. A* **2012**, *86*, 475–478.
28. Hamieh, T.; Gus'kov, V.Y. Surface Thermodynamic Properties of Styrene–Divinylbenzene Copolymer Modified by Supramolecular Structure of Melamine Using Inverse Gas Chromatography. *Chemistry* **2024**, *6*, 830-851. https://doi.org/10.3390/chemistry6050050.
29. Hamieh, T.; Gus'kov, V. Y. London Dispersive and Polar Surface Properties of Styrene–Divinylbenzene Copolymer Modified by 5-Hydroxy-6-Methyluracil using Inverse Gas Chromatography. *Preprints* **2025**, 2025040852. https://doi.org/10.20944/preprints202504.0852.v1.
30. Conder, J.R.; Locke, D.C.; Purnell, J.H. Concurrent solution and adsorption phenomena in chromatography. I. *J. Phys. Chem.* **1969**, *73*, 700–708. https://doi.org/10.1021/j100723a035.
31. Conder, J.R.; Purnell, J.H. Gas chromatography at finite concentrations. Part 2.—A generalized retention theory. *Trans. Faraday Soc.* **1968**, *64*, 3100–3011.
32. Conder, J.R.; Purnell, J.H. Gas chromatography at finite concentrations. Part 1.—Effect of gas imperfection on calculation of the activity coefficient in solution from experimental data. *Trans. Faraday Soc.* **1968**, *64*, 1505–1512. https://doi.org/10.1039/tf9686401505.
33. Sawyer, D.T.; Brookman, D.J. Thermodynamically based gas chromatographic retention index for organic molecules using salt-modified aluminas and porous silica beads. *Anal. Chem*. **1968**, *40*, 1847–1850. https://doi.org/10.1021/ac60268a015.
34. Hamieh, T.; Schultz, J. New approach to characterise physicochemical properties of solid substrates by inverse gas chromatography at infinite dilution. I. Some new methods to determine the surface areas of

some molecules adsorbed on solid surfaces. *J. Chromatogr. A* **2002**, *969*, 17–47. https://doi.org/10.1016/S0021-9673(02)00368-0.

35. Saint-Flour, C.; Papirer, E. Gas-solid chromatography. A method of measuring surface free energy characteristics of short carbon fibers. 1. Through adsorption isotherms. *Ind. Eng. Chem. Prod. Res. Dev.* **1982**, *21*, 337–341. https://doi.org/10.1021/i300006a029.
36. Saint-Flour, C.; Papirer, E. Gas-solid chromatography: Method of measuring surface free energy characteristics of short fibers. 2. Through retention volumes measured near zero surface coverage. *Ind. Eng. Chem. Prod. Res. Dev.* **1982**, *21*, 666–669. https://doi.org/10.1021/i300008a031.
37. Donnet, J.-B.; Park, S.; Balard, H. Evaluation of specific interactions of solid surfaces by inverse gas chromatography. *Chromatographia* **1991**, *31*, 434–440.
38. Chehimi, M.M.; Abel, M.-L.; Perruchot, C.; Delamar, M.; Lascelles, S.F.; Armes, S.P. The determination of the surface energy of conducting polymers by inverse gas chromatography at infinite dilution. *Synth. Met.* **1999**, *104*, 51–59.
39. Chehimi, M.M.; Pigois-Landureau, E. Determination of acid–base properties of solid materials by inverse gas chromatography at infinite dilution. A novel empirical method based on the dispersive contribution to the heat of vaporization of probes. *J. Mater. Chem.* **1994**, *4*, 741–745.
40. Brendlé, E.; Papirer, E. A new topological index for molecular probes used in inverse gas chromatography for the surface nanorugosity evaluation, 2. Application for the Evaluation of the Solid Surface Specific Interaction Potential. *J. Colloid Interface Sci.* **1997**, *194*, 217–224.
41. Brendlé, E.; Papirer, E. A new topological index for molecular probes used in inverse gas chromatography for the surface nanorugosity evaluation, 1. Method of Evaluation. *J. Colloid Interface Sci*. **1997**, *194*, 207–216.
42. Hamieh, T. Surface acid-base properties of carbon fibres. *Adv. Powder Technol*. **1997**, *8*, 279–289.
43. Le Vu, H.; Nguyen, S.H.; Dang, K.Q.; Pham, C.V.; Le, H.T. The Effect of Oxidation Temperature on Activating Commercial Viscose Rayon-Based Carbon Fibers to Make the Activated Carbon Fibers (ACFs). *Mater. Sci. Forum* **2020**, *985*, 171–176. https://doi.org/10.4028/www.scientific.net/MSF.985.171.
44. Liu, Y.; Gu, Y.; Wang, S.; Li, M. Optimization for testing conditions of inverse gas chromatography and surface energies of various carbon fiber bundles. *Carbon Lett.* **2023**, *33*, 909–920. https://doi.org/10.1007/s42823-023-00472-9.
45. Pal, A.; Kondor, A.; Mitra, S.; Thua, K.; Harish, S.; Saha, B.B. On surface energy and acid–base properties of highly porous parent and surface treated activated carbons using inverse gas chromatography. *J. Ind. Eng. Chem.* **2019**, *69*, 432–443. https://doi.org/10.1016/j.jiec.2018.09.046.
46. Hamieh, T. Study of the temperature effect on the surface area of model organic molecules, the dispersive surface energy and the surface properties of solids by inverse gas chromatography. *J. Chromatogr. A* **2020**, *1627*, 461372.
47. Hamieh, T.; Ahmad, A.A.; Roques-Carmes, T.; Toufaily, J. New approach to determine the surface and interface thermodynamic properties of H-β-zeolite/rhodium catalysts by inverse gas chromatography at infinite dilution. *Sci. Rep.* **2020**, *10*, 20894.
48. Hamieh, T. New methodology to study the dispersive component of the surface energy and acid–base properties of silica particles by inverse gas chromatography at infinite dilution. *J. Chromatogr. Sci.* **2022**, *60*, 126–142. https://doi.org/10.1093/chromsci/bmab066.
49. Hamieh, T. New Physicochemical Methodology for the Determination of the Surface Thermodynamic Properties of Solid Particles. *AppliedChem* **2023**, *3*, 229–255; https://doi.org/10.3390/appliedchem3020015.
50. Bauer, F.; Meyer, R.; Czihal, S.; Bertmer, M.; Decker, U.; Naumov, S.; Uhlig, H.; Steinhart, M.; Enke, D. Functionalization of porous siliceous materials, Part 2: Surface characterization by inverse gas chromatography. *J. Chromatogr. A* **2019**, *1603*, 297–310. https://doi.org/10.1016/j.chroma.2019.06.031.
51. Yao, Z.; Wu, D.; Heng, J.Y.Y.; Lanceros-Méndez, S.; Hadjittofis, E.; Su, W.; Tang, J.; Zhao, H.; Wu, W. Comparative study of surface properties determination of colored pearl-oyster-shell-derived filler using inverse gas chromatography method and contact angle measurements. *Int. J. Adhes. Adhes.* **2017**, *78*, 55–59. https://doi.org/10.1016/j.ijadhadh.2017.06.018.

52. Sidqi, M.; Balard, H.; Papirer, E.; Tuel, A.; Hommel, H.; Legrand, A. Study of modified silicas by inverse gas chromatography. Influence of chain length on the conformation of n-alcohols grafted on a pyrogenic silica. *Chromatographia* **1989**, *27*, 311–315. https://doi.org/10.1007/bf02321275.
53. Pyda, M.M.; Guiochon, G. Surface properties of silica-based adsorbents measured by inverse gas–solid chromatography at finite concentration. *Langmuir* **1997**, *13*, 1020–1025.
54. Hamieh, T. Serious irregularities and errors in the determination of the surface free energy and acido-basicity of MXene materials, Carbon, 2025, 120209, https://doi.org/10.1016/j.carbon.2025.120209.
55. Thielmann, F.; Baumgarten, E. Characterization of Microporous Aluminas by Inverse Gas Chromatography. *J. Colloid Interface Sci.* **2002**, *229*, 418–422. https://doi.org/10.1006/jcis.2000.6958.
56. Onjia, A.E.; Milonjić, S.K.; Todorović, M.; Loos-Neskovic, C.; Fedoroff, M.; Jones, D.J. An inverse gas chromatography study of the adsorption of organics on nickel- and copper-hexacyanoferrates at zero surface coverage. *J. Colloid Interface Sci.* **2002**, *251*, 10–17. https://doi.org/10.1006/jcis.2002.8372.
57. Przybyszewska, M.; Krzywania, A.; Zaborski, M.; Szynkowska, M.I. Surface properties of zinc oxide nanoparticles studied by inverse gas chromatography. *J. Chromatogr. A* **2009**, *1216*, 5284–5291. https://doi.org/10.1016/j.chroma.2009.04.094.
58. Ali, S.; Heng, J.; Nikolaev, A.; Waters, K. Introducing inverse gas chromatography as a method of determining the surface heterogeneity of minerals for flotation. *Powder Technol.* **2013**, *249*, 373–377. https://doi.org/10.1016/j.powtec.2013.09.004.
59. Shi, X.; Bertóti, I.; Pukánszky, B.; Rosa, R.; Lazzeri, A. Structure and surface coverage of water-based stearate coatings on calcium carbonate nanoparticles. *J. Colloid Interface Sci.* **2011**, *362*, 67–73. https://doi.org/10.1016/j.jcis.2011.06.025.
60. Hamieh , T. Comment on "New Method to Probe the Surface Properties of Polymer Thin Films by Two-Dimensional (2D) Inverse Gas Chromatography (iGC)", Langmuir, **2024**, *40* (44), 23562–23569, https://doi.org/10.1021/acs.langmuir.4c02483
61. Zhang, Y.; Wang, S.; Li, H.; Gong, M. Preparation of Toluene-Imprinted Homogeneous Microspheres and Determination of Their Molecular Recognition Toward Template Vapor by Inverse Gas Chromatography. *Chromatographia* **2017**, *80*, 453–461. https://doi.org/10.1007/s10337-017-3245-y.
62. Frauenhofer, E.; Cho, J.; Yu, J.; Al-Saigh, Z.Y.; Kim, J. Adsorption of hydrocarbons commonly found in gasoline residues on household materials studied by inverse gas chromatography. *J. Chromatogr. A* **2019**, *1594*, 149–159. https://doi.org/10.1016/j.chroma.2019.01.076.
63. Paloglou, A.; Martakidis, K.; Gavril, D. An inverse gas chromatographic methodology for studying gas-liquid mass transfer. *J. Chromatogr. A* **2017**, *1480*, 83–92. https://doi.org/10.1016/j.chroma.2016.12.034.
64. Hamieh, T. Inverse Gas Chromatography to Characterize the Surface Properties of Solid Materials. *Chem. Mater.* **2024**, *36*, 2231–2244. https://doi.org/10.1021/acs.chemmater.3c03091.
65. Hamieh, T. Some Irregularities in the Evaluation of Surface Parameters of Solid Materials by Inverse Gas Chromatography. *Langmuir* **2023, *39*, 17059–17070**. https://doi.org/10.1021/acs.langmuir.3c01649.
66. Hamieh, T. New Progress on London Dispersive Energy, Polar Surface Interactions, and Lewis's Acid–Base Properties of Solid Surfaces. *Molecules* **2024**, *29*, 949. https://doi.org/10.3390/molecules29050949.
67. Hamieh, T. London Dispersive and Lewis Acid-Base Surface Energy of 2D Single-Crystalline and Polycrystalline Covalent Organic Frameworks. *Crystals* **2024**, *14*, 148. https://doi.org/10.3390/cryst14020148.
68. Van Oss, C.J.; Good, R.J.; Chaudhury, M.K. Additive and nonadditive surface tension components and the interpretation of contact angles. *Langmuir.* **1988**, *4*, 884. https://doi.org/10.1021/la00082a018.
69. Dorris, G.M.; Gray, D.G. Adsorption of *n*-alkanes at zero surface coverage on cellulose paper and wood fibers. *J. Colloid Interface Sci.* **1980**, *77*, 353–362.